Journal of Applied Physics

A design for improved performance of interior permanent magnet synchronous motor for hybrid electric vehicle

Cite as: J. Appl. Phys. **99**, 08R308 (2006); https://doi.org/10.1063/1.2171953
Published Online: 20 April 2006

Seong Yeop Lim and Ju Lee

AIP Publishing

JOURNAL OF APPLIED PHYSICS **99**, 08R308 (2006)

A design for improved performance of interior permanent magnet synchronous motor for hybrid electric vehicle

Seong Yeop Lim[a] and Ju Lee
Department of Electrical Engineering, Hanyang University, 17 Haengdang-dong, Sungdong-gu, Seoul 133-791, Korea

(Presented on 3 November 2005; published online 20 April 2006)

This paper investigates the layout of a magnet shape on the performance of an interior permanent magnet (IPM) synchronous motor. The motor is used in a hybrid electric vehicle. The IPM motor is a pancake shaped motor that has permanent magnets inside the rotor. The motor acts as a rotational electrodynamic machine between the engine and transmission. The main purpose of redesigning the shape of the magnet is to improve the motor performance, especially the back-emf wave form, the efficiency, and the rated torque, within a restricted volume. The electromagnetic performance of the conventional model and the proposed design is analyzed using the finite element method. The theoretical results have been confirmed by comparing them with experimental results for the back-emf wave form, the torque versus current characteristics, and the motor efficiency. © *2006 American Institute of Physics*. [DOI: 10.1063/1.2171953]

As the recognition of the environmental problem has rapidly increased worldwide in the past few years, interest has grown in developing permanent magnet (PM) motors for nonpolluting electric vehicles (EV) and hybrid electric vehicles (HEV).[1] Many research papers have proposed the following PM configuration; surface-mounted PM (SPM), interior PM (IPM), and axial flux PM (AFPM) motors. Particularly, IPM motors have been intensively researched due to their high efficiency operation and the rotor of rugged construction. A number of researches have been reported in detail about the design technologies for improving the performance.[2–4]. Since the rotor structure has PMs embedded in the rotor core, the q-axis inductance of the IPM motor is greater than the d-axis inductance, and the reluctance torque can be effectively used in addition to the magnetic torque generated by the PMs. This guarantees that IPM motors offer a high efficiency and a high torque density. As a result, the magnet configuration is one of the critical design points for the application because the motor characteristics depend on how the magnets are buried in the rotor.

Although a significant amount of research has been undertaken regarding magnet configurations and performance improvements such as cogging torque and torque ripple reduction, no effort has been expended on reducing the harmonic components of the back-emf of the IPM motor for the soft type HEV. This study presents the optimum design of a motor configuration with an effective PM shape that improves the machine's performance, especially the back-emf wave form, the efficiency, and the rated torque. The HEV has a pancake shaped IPM motor that acts as a rotational electrodynamic machine between the engine and transmission. The proposed design in this paper has an effective PM configuration capable of generating a sinusoidal back-emf, which results in a simple current control method without any harmonic suppression schemes. This contributes to an improvement of the performance, especially the motor efficiency and the rated torque. The proposed design has a reverse C-shape (or arc-shape) PM configuration unlike conventional models that have lateral shape and V-shape magnets as shown in a previous study.[5] The electromagnetic performance of the conventional model and the proposed design is analyzed using the finite element method (FEM) analysis. Their results are confirmed with experimental results such as the back-emf wave form, the torque-current characteristics, and the motor efficiency.

Figure 1 shows schematic diagrams (1/8 model) and rotor cross sections of the proposed prototype IPM motor with the following features: (1) a concentrated or nonoverlapping winding comprising coils that are wound on each stator tooth, thus resulting in short end windings and thus a low copper loss and a reduced axial length; (2) a fractional ratio of the stator slot number (N_s) per rotor poles ($2p$), typically

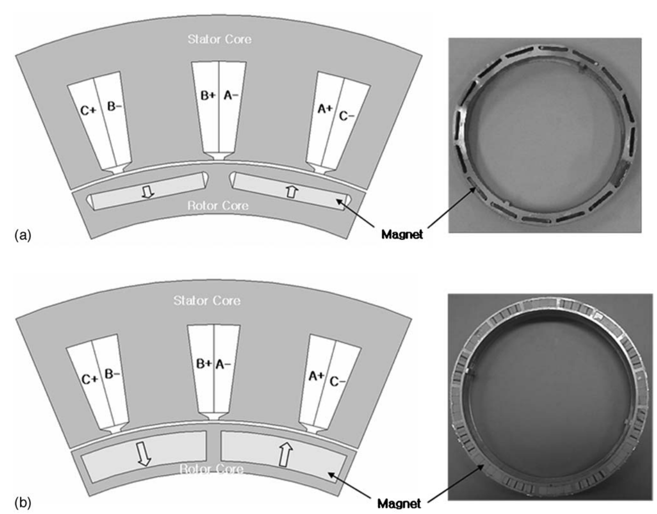

FIG. 1. Schematic diagrams and rotor cross sections of prototype motors. (a) Lateral magnet-type IPM motor (conventional model). (b) Arc-shape magnet-type IPM motor (proposed design).

[a]Electronic mail: lsyeop@ihanyang.ac.kr

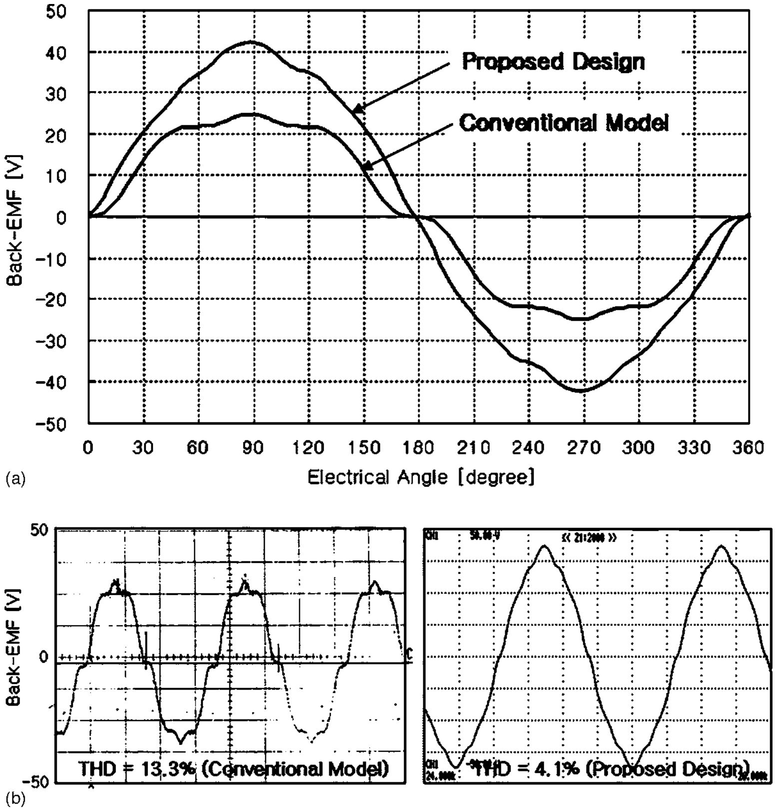

FIG. 2. Back-emf wave form of prototype motors. (a) Simulation results of back-emf. (b) Conventional model (measured). (c) Proposed design (measured).

24/16 ($N_s/2_p$), so as to minimize the cogging torque; (3) a maximum output power and torque of 12 kW and 80 N m, respectively. Figure 1(a) shows the lateral magnet-type IPM motor which is the conventional type of a magnet design. Figure 1(b) shows the proposed IPM motor with an arc-shape PM configuration. This is an optimal design which was obtained from a FEM analysis combined with the design of experiment (DoE).

When a concentrated winding is used, the back-emf wave form contains higher harmonics and the inductance difference between the q and d axes is lower than that of a distributed winding. Therefore, it is necessary to increase the inductance ratio L_q/L_d and make the back-emf wave form closer to a sinusoidal shape with total harmonics that are less than 5% of the fundamental component. To obtain an improved back-emf wave form and performance, three types of PM structure were examined in this paper. DoE in this study uses an orthogonal array of $L_{18}(3^5)$ and five design variables. The design variables consist of one magnetic characteristic variable and four geometrical variables related to the rare-earth magnet "Nd–Fe–B" embedded inside the rotor, as described in Table I. The electromagnetic performance of each case is analyzed using a two-dimensional FEM with reference to this orthogonal array. A restraint condition is to prevent the PM's demagnetization at an elevated temperature. The outline dimensions of the prototype motors are identical, except the rotor axial length.

TABLE I. Design variables for design of experiment (DoE).

Item		Level 1	Level 2	Level 3
A	Magnet Configuration (1pole)	Lateral shape 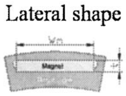	V-shape 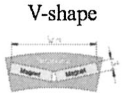	Arc-shape 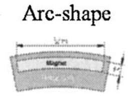
B	Magnet Specification	Br = 11.8kG iHc = 30kOe	Br = 13.2kG iHc = 26kOe	Br = 13.9kG iHc = 21kOe
C	Magnet Thickness (t)	4 mm	6 mm	8 mm
D	Magnet Width (Wm)	30 mm	33 mm	35 mm
E	Rotor Inner-Diameter	174 mm	172 mm	170 mm

The rotor overhang in the proposed design has an increase of 17.3% compared to the conventional model. The overhang effect was separately examined by a three-dimensional (3D) FE model for the overhang analysis. The overhang effect refers to the effect of fringing by which the effective area of the air gap is greater than the actual area. The linkage flux of the proposed design as shown in Fig. 1(b) due to the overhang effect is about 15.5% higher than that of the lateral magnet-type IPM motor, as shown in Fig. 1(a).

Figure 2 shows the calculated and measured results of the back-emf wave form at a speed of 1000 rpm taken for prototype IPM motors with lateral and arc-shape magnet structures. The calculated curvatures are in excellent agreement with the measured ones. In Figs. 2(b) and 2(c), the total harmonic distortion (THD) is obtained from a harmonics analysis in order to evaluate the improvement of the back-emf wave form quantitatively. The THD is defined as the ratio of the rms value of the total harmonics to the rms value of the fundamental frequency term. As shown in Fig. 2,

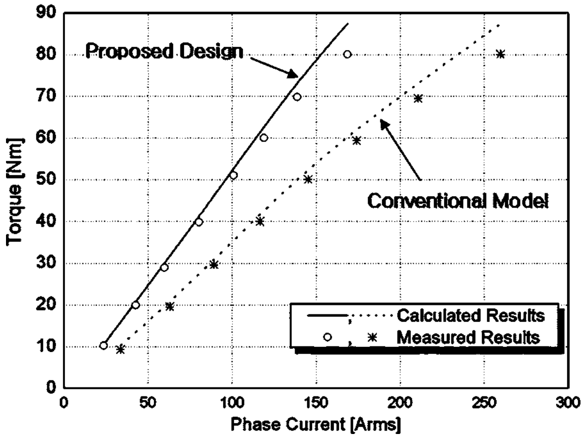

FIG. 3. Torque vs current characteristics of prototype motors.

whereas the back-emf wave form of the conventional model is greatly distorted, that of the proposed design is the closest to a sinusoidal in shape. From harmonics analysis, it was discovered that the conventional model (THD=13.3%) contained many higher harmonics than the proposed design (THD=4.1%). Furthermore, it was discovered that the effective air-gap flux was about 65% higher in the proposed design than in the conventional model, as shown in Fig. 2(a). This is because the magnet type was changed from the lateral shape to the arc shape. Also, high-energy product magnets ($BH_{\max}$=42 MG Oe) and the overhang effect were provided to the proposed design. The large increment of the effective air-gap flux enables a motor to have higher output torque density and smaller stator copper losses, which results in higher motor efficiency.

Figure 3 shows the calculated and measured output torque against phase current at a speed of 500 rpm. The measured results were obtained from a steady-state output characteristic experiment. The similarity between the results is good. However, as the current is larger, the experimental values of the rated torque are decreased. This is mainly related to the magnet operating temperature; it is slightly higher than the calculated one, giving a lower remanence (B_r) for the Nd–Fe–B magnets than the ones used in the FEM analysis. The maximum torque (80 N m) for the arc-shape magnet-type IPM motor was generated at about 170 A, whereas with a lateral magnet-type IPM motor, the maximum torque was obtained at about 260 A. It was discovered that the output torque density at approximately 170 A was about 33.3% higher in the proposed design than in the conventional model, as shown in Fig. 3.

Figure 4 shows experimental results for two motor efficiency regions (87% over). The operating region for a motor efficiency greater than 90% was a minimum of 80% wider in the proposed design than in the conventional model. Also, the maximum efficiency was about 3% higher in the proposed design than in the conventional model. The maximum efficiency region (93% over) was displayed within the main operating region of the IPM motor for the soft type HEV.

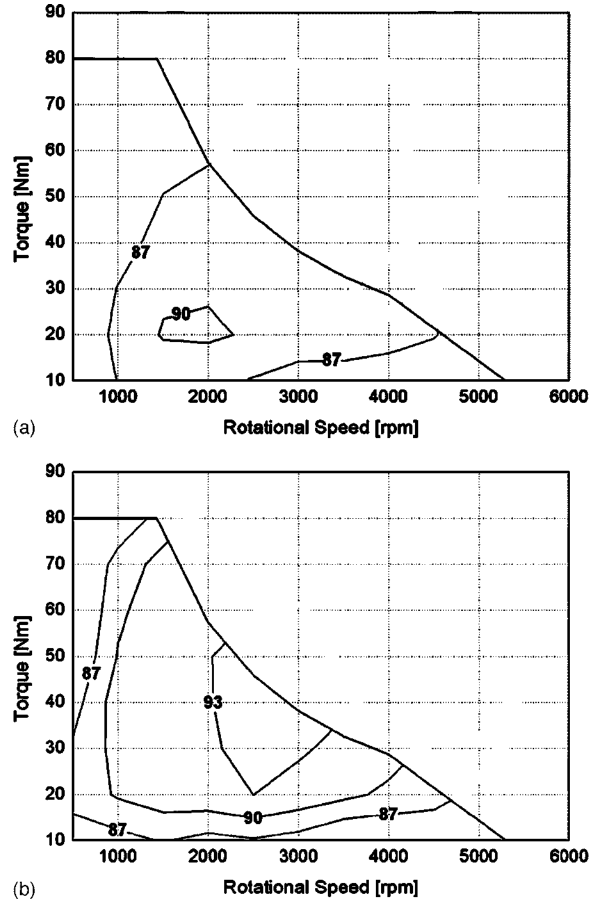

FIG. 4. Motor efficiency characteristics of prototype motors. (a) Lateral magnet-type IPM motor (conventional model). (b) Arc-shape magnet-type IPM motor (proposed design).

From simulations and experiments using two prototype motors, we confirmed the following performance improvement with regards to the optimum motor configuration of the IPM motor used for the HEV.

(1) The proposed PM configuration was effective in generating good sinusoidal back-emf wave form with total harmonics that are less than 5% of the fundamental component.
(2) By adopting the proposed PM configuration, the region with a motor efficiency over 90% was a minimum of 80% wider than that of lateral PM configuration. Also, the maximum efficiency was about 3% higher in the proposed design than in the conventional model. The rated torque generated at a constant current of approximately 170 A was about 33.3% higher than that of the conventional model.

[1]J. W. Park *et al.*, IEEE Trans. Ind. Appl. **37**, 1754 (2001).
[2]T. Ohnishi and N. Takahashi, IEEE Trans. Magn. **36**, 3537 (2000).
[3]Z. Q. Zhu *et al.*, IEEE Trans. Magn. **39**, 3238 (2003).
[4]J. R. Hendershot Jr. and T. J. E. Miller, *Design of Brushless Permanent-Magnet Motors* (Clarendon, New York, 1994).
[5]K.-J. Lee *et al.*, J. Appl. Phys. **97**, 10Q505 (2005).